IEEE Access
Multidisciplinary : Rapid Review : Open Access Journal

Received April 24, 2018, accepted June 8, 2018, date of publication June 20, 2018, date of current version July 12, 2018.

Digital Object Identifier 10.1109/ACCESS.2018.2849093

Nearly Non-Coupling Coil Array Allowing Many Independent Channels for Magnetic Communication

HAN-JOON KIM[1], (Student Member, IEEE), KYUNGTAE KIM[1], (Student Member, IEEE), SUNGMIN HAN[1], (Student Member, IEEE), DONG-WOOK SEO[2], AND JI-WOONG CHOI[1], (Senior Member, IEEE)

[1]Department of Information and Communication Engineering, Daegu Gyeongbuk Institute of Science and Technology, Daegu 771-873, South Korea
[2]Department of Radio Communication Engineering, Korea Maritime and Ocean University, Busan 49112, South Korea

Corresponding author: Ji-Woong Choi (jwchoi@dgist.ac.kr)

This work was supported in part by the Bio & Medical Technology Development Program of the National Research Foundation of Korea (NRF) through the Ministry of Science, ICT and Future Planning under Grant NRF-2017M3A9G8084463, in part by the Basic Science Research Program through NRF, Ministry of Science, ICT and Future Planning, under Grant NRF-2017R1E1A1A01077393, and in part by the Robot Industry Fusion Core Technology Development Project of the Ministry of Trade, Industry & Energy of Korea under Grant 10052980.

ABSTRACT Crosstalk between coil array components in magnetic systems has to be minimized to achieve enhanced performance, such as high data rate, high-power transfer efficiency, and simultaneous wireless information and power transfer. This paper presents a scalable non-coupling coil array composed of perpendicularly arranged quadrupole loop coils. The proposed coil array permits the number of fully or nearly independent channel streams to be increased to meet user's requirements, unlike conventional coil arrays which have a limited number of channel streams. The proposed non-coupling coil array structure is investigated by theoretical analysis and 3-D electromagnetic simulation, and the performance of the proposed non-coupling coil array is verified with a prototype implementation. The proposed coil array shows relatively high signal-to-interference and noise power ratio of around 20 dB even at the three times further distance of a coil diameter.

INDEX TERMS Crosstalk cancellation, magnetic communication, non-coupling coil array, wireless power transfer.

I. INTRODUCTION

Magnetic communication and wireless power transfer (WPT) technologies can be applied to a wide number of applications, ranging from mobile devices to specialized applications for high permittivity environments such as underground, underwater, and inside of biological tissues. However, the conventional magnetic communication and WPT have limitations such as short transmission range, power transfer efficiency (PTE) drop due to misalignment, and low data rate. Many research groups have presented various approaches to solve the limitations. Transmission range extension can be achieved by magnetic resonance, magnetic relay, and ferrite-loaded coils. Low PTE due to the misalignment can be compensated by using specialized coil structure, electrical compensation, and metamaterials. Lastly, the data rate can be improved using high and wide carrier frequency bands, efficient modulation schemes, and magnetic multi-input and multi-output (MIMO) [1]. Neuro-prosthesis implantable devices such as a cochlear implant, artificial retina, and prosthetic hand are typical applications to require simultaneous information and power transfer (SWIPT), and high rate communication for high-resolution data transmission. Conventional communication and power transmission technologies have difficulty supporting a simultaneous data-rate and PTE that is sufficient to mimic the performance of human body functions [2]. Many research groups have applied various approaches as previously mentioned to achieve the high data rate and efficient WPT for the implantable devices. Yakovlev *et al.* [3] proposed mid-field coupling operating in the low-GHz range to obtain high PTE for millimeter-sized implantable devices. In this case, the high data rate is an incidental outcome of the mid-field coupling system using high carrier frequency. Kiani and Ghovanloo [2] applied pulse based modulation with a dual-band inductive link to obtain both high data rate and high PTE simultaneously.

Although there are also many methods to achieve high data rate and SWIPT, the achievable data rate is still not enough to reach the similar performance of the human organs. Multiple channel or multiple band systems using coil arrays could be a one of possible ways to achieve high data rate and high PTE simultaneously. There are a few research groups which have employed coil arrays in magnetic communication and WPT systems to achieve enhanced performance, including high data rate [4]–[8], high PTE [9]–[13], and SWIPT [14]–[17]. In some cases when using the coil array, crosstalk or cross-coupling between the array components has occurred, and this crosstalk is considered to be a critical problem since it leads to significant interference and power leakage. Reduction of this crosstalk can be achieved by various methods such as electrical compensation [18], or the use of multiple frequencies [7], [15], [17], and unique structures [6], [8], [12], [17]. For example, Cui added additional impedance to a receiver to compensate the power loss caused by crosstalk between multiple receivers [18]. For static situations, adding impedance is a practical way of removing the effects of crosstalk. The multiple carrier schemes can increase data rate and SWIPT by reducing crosstalk, at the cost of additional frequency resources [7], [15], [17]. However, when high interference is induced by the powering signal, the multiple carrier methods are not sufficient to prevent crosstalk. In the high interference situation, the unique coil structure can be an alternative solution to reduce crosstalk in the physical domain. For implantable systems, Jow applied both multiple carriers and a unique coil structure consisting of an orthogonal coil array and a quadrupole loop coil to reduce the crosstalk in the SWIPT system [17]. The orthogonal coil array, which is one of the popular coil structures for reducing crosstalk, has been applied to various systems including MIMO [5], magnetic beamforming [12], and SWIPT systems [14]. A coplanar overlapped coil array was also able to achieve separated channel streams up to 4 × 4 MIMO, using a three dimensional (3D) structure forming a pyramid [8]. However, most coil arrays cannot easily increase the number of channel streams, because they require additional frequency resources and have structural limitations to increase the channels. For example, Guo and Sun [7], Zhou *et al.* [15], Jow and Ghovanloo [17], and Cui *et al.* [18] require additional resources for multiple independent channels and the maximum number of channels which can be provided by Guttula [5], Kim *et al.* [6], Tal *et al.* [8], and Kisseleff *et al.* [12] are four or the less due to structural limitations. To mitigate these problems, this paper presents a nearly non-coupling coil array that consists of quadrupole loop coils arranged perpendicularly to each other, enabling an easier extension of the number of channel streams. The proposed coil array has advantages as follows.

1) The proposed coil array can increase the number of independent channels as much as user's requirement on a two dimensional plane. Therefore, it can be easily applied to implantable devices or mobile devices which require miniaturization.

2) The proposed coil array does not require extra resources such as frequency bands, RLC components, and power to intentionally reduce the coupling for extension of the number of channels.

In the following, Section II presents the principle of the proposed coil array and Section III verifies the performance of the proposed coil array via simulation and measurement. Lastly, Section IV provides the summary and potential of the proposed method.

II. CROSSTALK CANCELLATION USING A SCALABLE COIL PATTERN

A. A CONVENTIONAL CROSSTALK-FREE COIL ARRAY

In a previous study, we proposed a non-coupling coil array using a heterogeneous multi-pole loop coil array with a crosstalk cancellation plane [6]. The proposed crosstalk cancellation method intentionally created full decoupling using multiple magnetic fields which were induced by opposite currents (i.e., $I_1 = -I_2$) with the same magnitude at a specific distance from coils. Figure 1 is a primary non-coupling array which consists of a circular loop (Fig. 1 (A)) and a quadrupole loop (Fig. 1 (B)). The coil B produces two magnetic fields of the same field strength but in opposite directions, and the total magnetic field is equal to 0 at the same distance from the center of each loop. A quadrupole loop has been used in the inductor design of the circuit to reduce crosstalk [19]. Since a specific analysis of corsstalk reduction was not provided in [19], this paper performs the detailed analysis on the crosstalk cancellation using the quadrupole loop. The magnetic field from each circular loop is expressed by [20]

$$H_i = \frac{I_i N_i}{2\pi} \frac{1}{\sqrt{(a_i+\rho_i)^2 + z_i^2}} \times \left[K(k_i) + \frac{a_i^2 - \rho_i^2 - z^2}{(a_i^2 - \rho_i)^2 + z^2} E(k_i) \right] \quad (1)$$

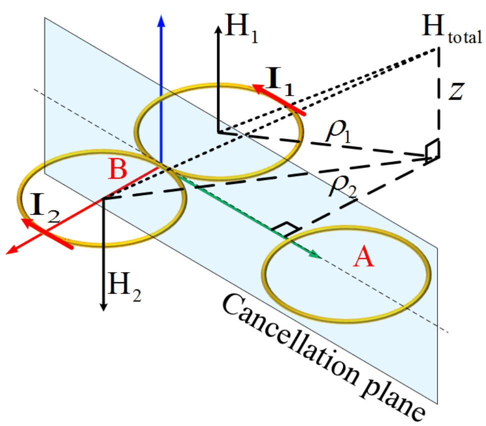

FIGURE 1. The primary coil array pattern for crosstalk cancellation.

where a_i, N_i are the radius and number of turns of each circular loop i, respectively. ρ_i is the distance from the center of each circular loop in the XY plane, and z is the height of a measurement point. Defining

$$k_i^2 = \frac{4a_i\rho_i}{(a_i+\rho_i)^2+z^2}, \tag{2}$$

where $K(k_i)$ and $E(k_i)$ are the complete elliptic integrals of the first and second kind which were tabulated by Dwight as [21]

$$K(k_i) = \int_{\theta=0}^{\frac{\pi}{2}} \frac{d\theta}{\sqrt{1-k^2\sin^2\theta}}, \tag{3}$$

and

$$E(k_i) = \int_{\theta=0}^{\frac{\pi}{2}} \sqrt{1-k^2\sin^2\theta}\,d\theta. \tag{4}$$

Then, a total magnetic field $\mathrm{H_{total}}$ can be obtained by $\mathrm{H_{total}} = \mathrm{H_1} + \mathrm{H_2}$. The non-coupling coil array has to satisfy the following condition. When the center of coil A is located in the cancellation plane of coil B, coils A and B have no coupling. Figure 1 shows the cancellation in a two-dimensional (2D) plane using the H-field. Similarly, it can be easily extended to a 3D space. However, the coil patterns in Fig. 2 have a few weaknesses. Figure 2 (a) shows the cancellation planes created using heterogeneous multi-pole loops which have parallel linked circular loops and Figure 2 (b) shows the cancellation plane using an unbalanced quadrupole loop with the primary coil pattern. Both Fig. 2 (a) and (b) are presented in [6]. They are not easy to arrange efficiently in limited space since they have to be placed in line to maintain the crosstalk cancellation condition. Furthermore, it is hard to design heterogeneous coils to expand as much as the user's required number of channel streams meeting the crosstalk cancellation condition. Even if the coil array consists of a repetition of primary coil pattern as in Fig. 2 (c), it cannot guarantee separate channel streams, due to significant interference between the circular coil loops. The heterogeneous coils may also cause a gain difference between channels, leading to signal to interference and noise power ratio (SINR) degradation. We have also provided a method to prevent the SINR degradation using coil tuning for each heterogeneous coil [22]. However, the coil tuning procedure involves high design complexity. This paper proposes a new nearly non-coupling coil array which mitigates the above limitations while preserving crosstalk cancellation.

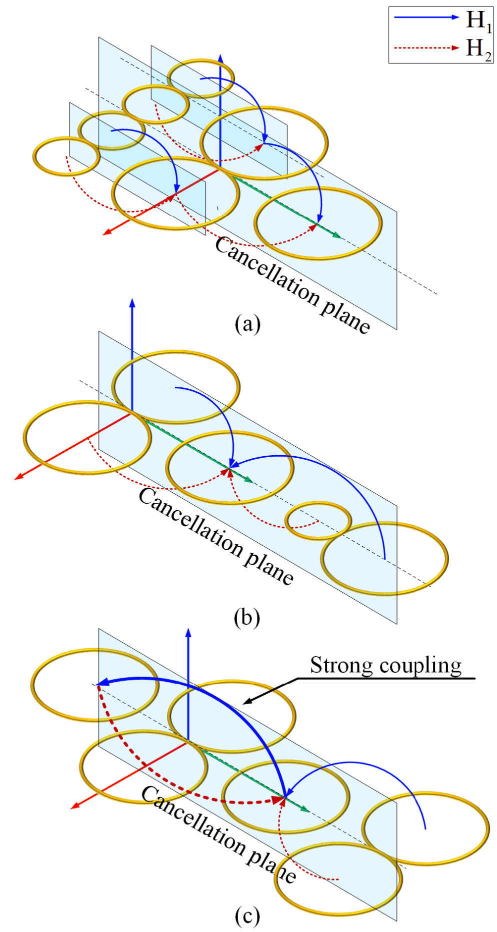

FIGURE 2. Expanded coil array using previous coil pattern (a) and (b) example of 3 channels cases, (c) example of 4 channels case using repeated primary coil pattern.

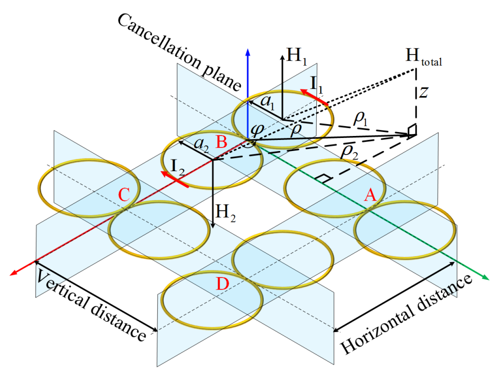

FIGURE 3. Proposed nearly non-coupling scalable coil array.

B. PROPOSED NEARLY NON-COUPLING SCALABLE COIL ARRAY

Using the same property of the previous coil array, a scalable non-coupling coil array can be formed by arranging quadrupole loop coils perpendicular to each other, as seen in Fig. 3. The proposed coil array can overcome the drawbacks of the previous heterogeneous coil pattern. It can satisfy the previous cancellation condition using a perpendicular arrangement (e.g., coils A and B, or A and D). Figure 4 shows the geometric relationship between the two perpendicularly arranged quadrupole loop coils on the XY plane depending on ϕ, which is the angle between the two quadrupole loops. ρ_{ji} is the distance from the circular loop i of coil B to the circular loop j of coil A. $\mathrm{H_{ji}}$ is magnetic fields at the circular loop j of coil A from the circular loop i of coil B and $\mathrm{H_j}$ is the aggregated magnetic field at the circular loop j of coil A. The magnetic fields are calculated (1) depending on the angle ϕ from 0° to 180° at the quadrupole loop coil A, as shown

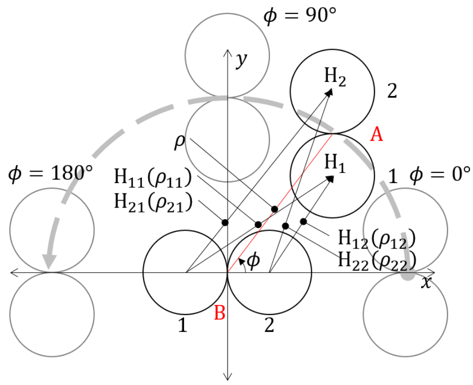

FIGURE 4. Geometric relationship between perpendicularly arranged quadrupole loop coils.

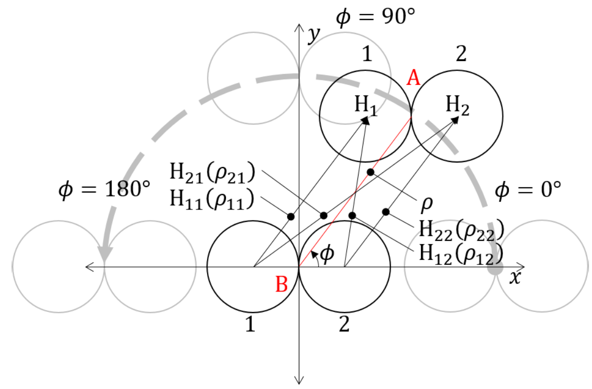

FIGURE 6. Geometric relationship between diagonally arranged quadrupole loop coils.

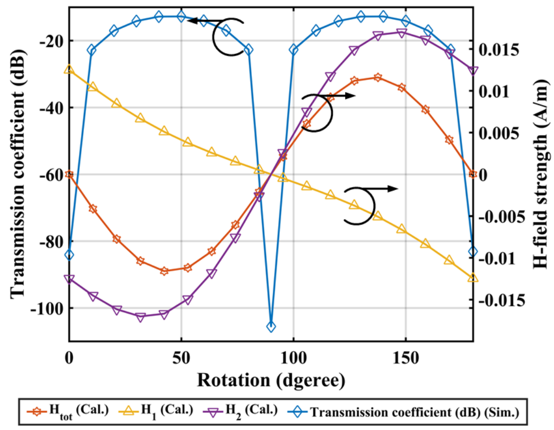

FIGURE 5. Tendency of summation of magnetic fields depending on angle between quadrupole loop coils in perpendicular arrangement.

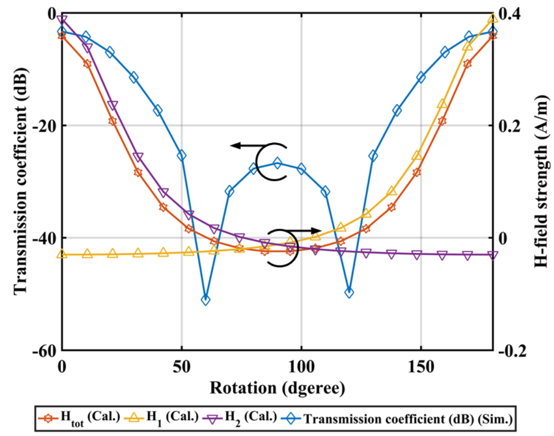

FIGURE 7. Tendency of summation of magnetic fields depending on the angle between diagonally arranged quadrupole loop coils.

in Fig. 5, which presents the plotted analysis results of the magnetic fields and transmission coefficient from the 3D EM simulation. The magnetic fields at the center of circular loop 1 and circular loop 2 of coil A are plotted by the purple line and yellow line, respectively. The total magnetic field at coil A is described by the orange line which is a summation of the purple line and yellow line. The total magnetic field strength (orange line) becomes 0 when the angles between the two quadrupole loops ϕ are 0°, 90° and 180° as shown in Fig. 5. Zero magnetic field strength means that coil A does not have an induced current from the coil B. Therefore, these coils cannot produce any coupling between array components. The analysis result was verified by 3D EM simulation using the same conditions. Figure 5 shows the transmission coefficient between the two quadrupole loop coils, which has a minimum value at the same angles as those in the analysis result. Since the low transmission coefficient means weak coupling between the two quadrupole loop coils, the tendency of the EM simulation result matches the analysis result well.

However, the pair of diagonally-arranged coils cannot satisfy the crosstalk cancellation (e.g., coils A and C, or B and D). To find the perfect crosstalk cancellation condition between the array components, the diagonally arranged case was also investigated using the same analysis procedure as the perpendicular case. Figure 6 shows the geometric relationship between the two diagonally located quadrupole loop coils depending on the angle ϕ between the two coils. The diagonally arranged case has particular angles that can cancel the crosstalk at $\phi = 60°$ or 120°, as also shown in the simulation in Fig. 7.

For complete crosstalk cancellation, the quadrupole loop coils need to be perpendicularly arranged in a rectangle, i.e., 90°, while they have to form an angle of 60° or 120° for diagonally arranged coils. However, it is not easy to keep both conditions and implement a complete non-coupling coil array, due to the geometric limitations. Thus, this paper presents a nearly non-coupling coil array which is arranged in a square form (i.e., 90° as seen in Fig. 3 as a sub-optimum solution for easy design of scalable arrays). The proposed coil array partially allows crosstalk between the diagonally arranged coils that form an angle of 45°. However, even if the proposed coil array has partial crosstalk, it may provide sufficient crosstalk cancellation. The effect of partially allowed crosstalk from simulation and measurement is discussed in Section III.

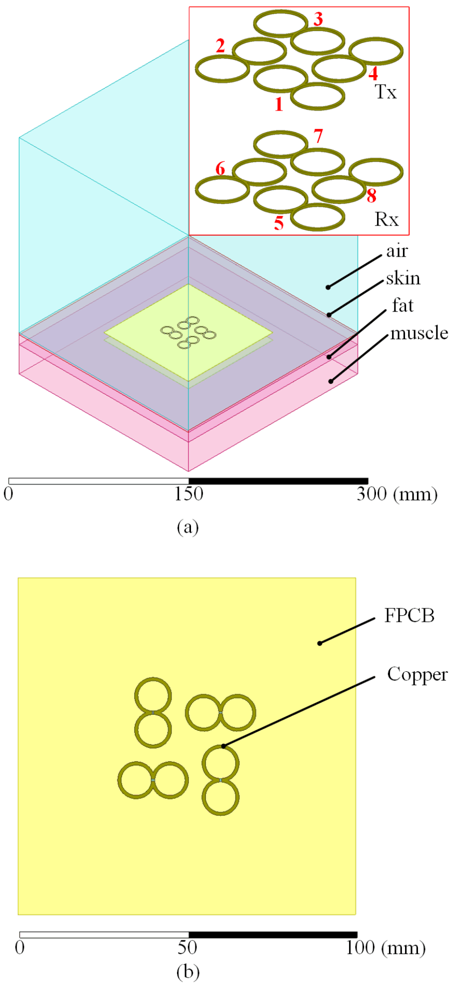

FIGURE 8. 3D EM simulation model (a) 3-layered phantom and pair of coil array, (b) coil array on the FPCB.

TABLE 1. Parameters of simulation model.

Medium	Permittivity	Conductivity (simens/m)	Loss tangent	Thickness (mm)
Skin (dry)	285.25	0.24	1.11	1.97
Fat	11.82	0.03	3.40	5.00
Muscle	138.44	0.63	6.02	30

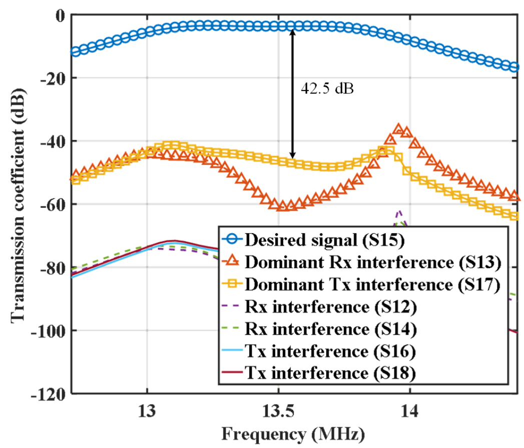

FIGURE 9. Simulation results of selected channels in the proposed coil array.

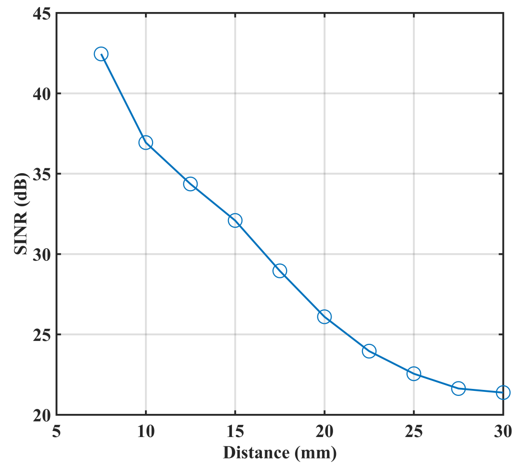

FIGURE 10. SINR depending on transmission distance at 13.56MHz.

III. SIMULATION & MEASUREMENT RESULTS

The proposed coil array has the potential to provide a high data rate and simultaneous power transmission capable of supporting neuro-prosthesis devices. This section presents the channel characteristics of the proposed method assuming an embedded situation inside subcutaneous fat, via simulation and measurement results. The 3D electromagnetic (EM) simulation model considered an neuro-prosthesis devices implanted under the skin with human tissue (a 3-layered phantom model including skin, fat, and muscle layer) as shown in Fig. 8. This corresponds to a 4×4 near-field magnetic MIMO system with the proposed coil array tuned at 13.56 MHz. The electric characteristics and thickness of the layers were also taken into account at 13.56 MHz [23]–[25], as shown in Table 1. The transmit coil array (coils 1 to 4) was placed on the surface of the skin layer and the receiver coil array (coils 5 to 8) were embedded in the subcutaneous fat as shown in Fig. 8 (a). The specific physical dimensions of the simulation model were as follows: the size of the coil array was 40 mm $\times$ 40 mm; the diameter of each circle was 10 mm; vertical and horizontal distance was 15 mm; and transmission distance was 7.5 mm to consider average thickness of human tissues. Figure 9 shows the transmission coefficient of a selected channel (S15) of the proposed coil array, and SYX denotes S-parameters from coil X to coil Y. As mentioned in Section II, perpendicularly arranged coils guarantee enough isolation between channel streams. Inevitably, dominant interference signals are induced from diagonally arranged coils (e.g., S13 and S17) which cannot satisfy the cancellation condition. Nevertheless, one can observe that the proposed coil array achieves around 42.5 dB SINR at 13.56 MHz under the partial cancellation condition at a short transmission distance smaller than the coil

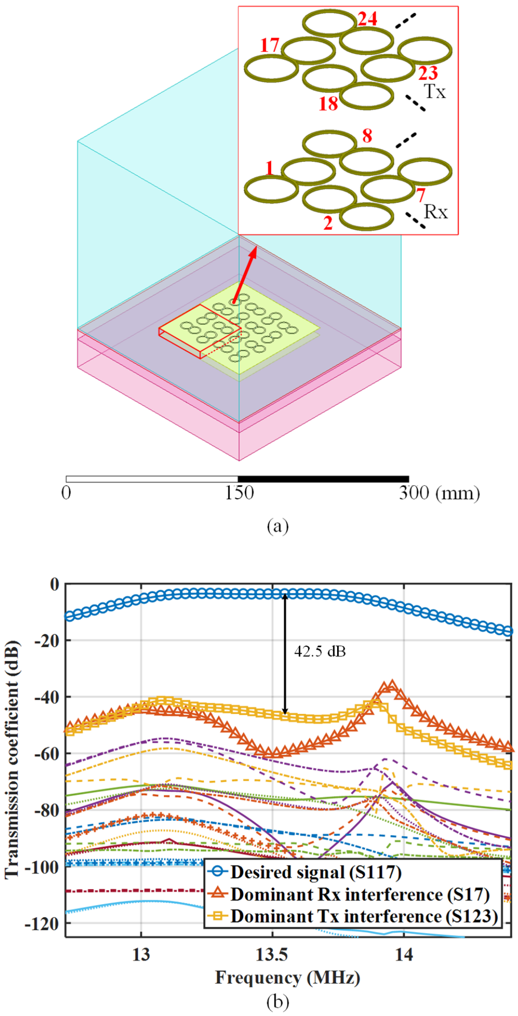

FIGURE 11. 3D EM simulation model (a) 16 × 16 coil array, (b) simulation results of selected channels in the 16 × 16 coil array.

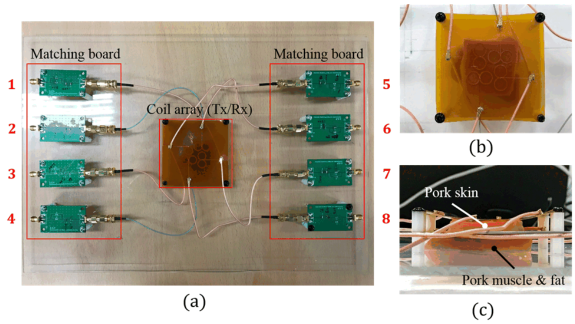

FIGURE 12. Proposed coil array testbed (a) whole system, (b) top view of measurement setting, (c) side view of measurement setting.

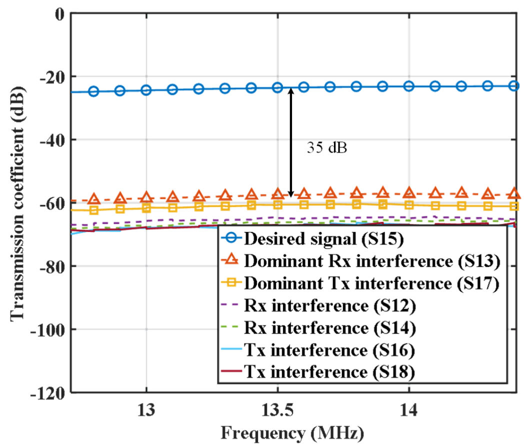

FIGURE 13. Measurement results of selected channels in the proposed coil array.

diameter as shown in Fig. 9. Note that 42.5 dB SINR is good enough for most M-ary QAM from 4-QAM to 1024-QAM to achieve fewer than 10^{-7} BER in the presence of additive white Gaussian noise [26]. Therefore, the proposed method can achieve enough BER for high-order modulation, allowing high data rate transmission. When the transmission distance is larger than the coil diameter, the SINR of the proposed coil array is decreased due to dominant interference from the diagonally located coils. Figure 10 presents the SINR depending on the transmission distance via numerical simulation. The SINR over 20 dB can be achieved at the three times further distance of the coil diameter. Even if the partial crosstalk decreases the SINR, the proposed method can achieve enough BER of 10^{-7} for 64-QAM [26]. To show the extendibility of the proposed coil array, we present 16 × 16 coil array simulation results using the same environment as the previous simulation, as shown Fig. 11 (a). Figure 11 (b) shows similar tendency to the case of 4 × 4 array for the dominant results, indicating that the proposed coil array can support nearly identical scalable channel streams as much as user's requirement. Among the selected channel streams, we only marked important channel streams in the legend, such as the desired signal channel stream (S117), dominant interference from the receiver array (S17) and, dominant interference from the transmitter array (S123).

The proposed coil array was then fabricated in copper on the flexible printed circuit board (FPCB) following the physical dimensions used in the 3D simulation model. The FPCB is a proper substrate for implantable devices since it is robust, thin and flexible [27]. The measured media was composed of 3 layers like the simulation model, using a pork tissue sample, which has electrical characteristics similar to human tissues [28]. The transmit coil array was located on the pork skin tissue, and the receiver coil array was inserted in the fat layer as shown in Fig. 12. The measurements were performed using a Keysight vector network analyzer E5061B, and the results are shown in Fig. 13. In the measurement results, the proposed array provided a sufficient channel gain of around 35 dB of SINR. The measurement results show a lower transmission coefficient than the simulation result, since there were additional losses caused by the connecting cable and impedance matching environment. However, the measurement results had almost the same tendency as the simulation results in Fig. 9. Both results show that although the diagonal signal path causes the largest interference among the interference paths, the desired signal path can achieve sufficient SINR for high data rate communications.

IV. CONCLUSION

We proposed a nearly non-coupling coil array using perpendicularly arranged quadrupole loop coils. The proposed coil array can easily increase the number of channels, to meet a user's requirement, by repeating the proposed pattern. We investigated the crosstalk cancellation of the proposed coil array depending on the angle between the two quadrupole loop coils, and the crosstalk cancellation condition of each arrangement was determined by theoretical analysis. Then, the channel characteristics of the proposed coil array were provided by simulation and measurement, based on neural-prosthesis implantable devices under the skin. The proposed coil array provided a sufficient SINR even though it had partial crosstalk between the parallel arranged coils. The proposed scheme can be applied to any applications which need multiple independent channel streams to obtain high data rate, high PTE, and SWIPT.

REFERENCES

[1] H. -J. Kim, H. Hirayama, S. Kim, K. J. Han, R. Zhang, and J.-W. Choi, ''Review of near-field wireless power and communication for biomedical applications,'' *IEEE Access*, vol. 5, pp. 21264–21285, 2017, doi: 10.1109/ACCESS.2017.2757267.

[2] M. Kiani and M. Ghovanloo, ''A 13.56-Mbps pulse delay modulation based transceiver for simultaneous near-field data and power transmission,'' *IEEE Trans. Biomed. Circuits Syst.*, vol. 9, no. 1, pp. 1–11, Feb. 2015, doi: 10.1109/TBCAS.2014.2304956.

[3] A. Yakovlev, S. Kim, and A. Poon, ''Implantable biomedical devices: Wireless powering and communication,'' *IEEE Commun. Mag.*, vol. 50, no. 4, pp. 152–159, Apr. 2012, doi: 10.1109/MCOM.2012.6178849.

[4] H. Nguyen, J. I. Agbinya, and J. Devlin, ''Channel characterisation and link budget of MIMO configuration in near field magnetic communication,'' *Int. J. Electron. Telecommun.*, vol. 59, no. 3, pp. 255–262, Sep. 2013, doi: 10.2478/eletel-2013-0030.

[5] R. B. Gottula, ''Discrete-time implementation, antenna design, and MIMO for near-field magnetic induction communications,'' M.S. thesis, Dept. Elect. Comput. Eng., Brigham Young Univ., Provo, UT, USA, Jul. 2012.

[6] H.-J. Kim, J. Park, K.-S. Oh, J.-P. Choi, and J.-W. Choi, ''Near-field magnetic induction MIMO communication using heterogeneous multipole loop antenna array for higher data rate transmission,'' *IEEE Trans. Antennas Propag.*, vol. 64, no. 5, pp. 1952–1962, May 2016, doi: 10.1109/TAP.2016.2539371.

[7] H. Guo and Z. Sun, ''Increasing the capacity of magnetic induction communication using MIMO coil-array,'' in *Proc. Global Commun. Conf. (GLOBECOM)*, Washington, DC, USA, Dec. 2016, pp. 1–6.

[8] N. Tal, Y. Morag, and Y. Levron, ''Magnetic induction antenna arrays for MIMO and multiple-frequency communication systems,'' *Prog. Electromagn. Res. C*, vol. 75, pp. 155–167, Jul. 2017, doi: 10.2528/PIERC17030703.

[9] J. Jadidian and D. Katabi, ''Magnetic MIMO: How to charge your phone in your pocket,'' in *Proc. Annu. Int. Conf. MobiCom Comput. Netw.*, Maui, HI, USA, Sep. 2014, pp. 495–506.

[10] L. Shi, Z. Kabelac, D. Katabi, and D. Perreault, ''Wireless power hotspot that charges all of your devices,'' in *Proc. Annu. Int. Conf. MobiCom Comput. Netw.*, Paris, France, Sep. 2015, pp. 2–13.

[11] B. H. Waters, B. J. Mahoney, V. Ranganathan, and J. R. Smith, ''Power delivery and leakage field control using an adaptive phased array wireless power system,'' *IEEE Trans. Power Electron.*, vol. 30, no. 11, pp. 6298–6309, Dec. 2015, doi: 10.1109/TPEL.2015.2406673

[12] S. Kisseleff, I. F. Akyildiz, and W. Gerstacker, ''Beamforming for magnetic induction based wireless power transfer systems with multiple receivers,'' in *Proc. IEEE Global Commun. Conf. (GLOBECOM)*, San Diego, CA, USA, Dec. 2015, pp. 1–7.

[13] K. Kim, H.-J. Kim, and J.-W. Choi, ''Magnetic beamforming with non-coupling coil pattern for high efficiency and long distance wireless power transfer,'' in *Proc. IEEE Wireless Power Transf. Conf.*, Taipei, Taiwan, May 2017, pp. 1–4.

[14] S. Kisseleff, I. F. Akyildiz, and W. H. Gerstacker, ''Magnetic induction-based simultaneous wireless information and power transfer for single information and multiple power receivers,'' *IEEE Trans. Commun.*, vol. 65, no. 3, pp. 1396–1410, Mar. 2017, doi: 10.1109/TCOMM.2016.2646684.

[15] M. Zhou, M. R. Yuce, and W. Liu, ''A non-coherent DPSK data receiver with interference cancellation for dual-band transcutaneous telemetries,'' *IEEE J. Solid-State Circuits*, vol. 3, no. 9, pp. 2003–2012, Sep. 2008, doi: 10.1109/JSSC.2008.2001881.

[16] G. Simard, M. Sawan, and D. Massicotte, ''High-speed OQPSK and efficient power transfer through inductive link for biomedical implants,'' *IEEE Trans. Biomed. Circuits Syst.*, vol. 4, no. 3, pp. 192–200, Jun. 2010, doi: 10.1109/TBCAS.2009.2039212.

[17] U.-M. Jow and M. Ghovanloo, ''Optimization of data coils in a multi-band wireless link for neuroprosthetic implantable devices,'' *IEEE Trans. Biomed. Circuits Syst.*, vol. 4, no. 5, pp. 301–310, Oct. 2010, doi: 10.1109/TBCAS.2010.2049491.

[18] D. Cui, T. Imura, and Y. Hori, ''Cross coupling cancellation for all frequencies in multiple-receiver wireless power transfer systems,'' in *Proc. Int. Conf. Antennas Propag. (ISAP)*, Okinawa, Japan, Oct. 2016, pp. 48–49.

[19] A. Poon, A. Chang, H. Samavati, and S. S. Wong, ''Reduction of inductive crosstalk using quadrupole inductors,'' *IEEE J. Solid-State Circuits*, vol. 44, no. 6, pp. 1756–1764, Jun. 2009, doi: 10.1109/JSSC.2009.2020525.

[20] C. R. Paul, ''The concept of 'loop' inductance,'' in *Inductance: Loop and Partial*, 3rd ed. Hoboken, NJ, USA: Wiley, 2011, ch. 4, pp. 117–194.

[21] H. B. Dwight, ''Elliptic functions,'' in *Tables of Integrals and Other Mathematical Data*, 4th ed. New York, NY, USA: Macmillan, 1961, ch. 9, pp. 168–173.

[22] H.-J. Kim and J.-W. Choi, ''Crosstalk-free magnetic MIMO communication using heterogeneous antenna array,'' in *Proc. URSI Asia–Pacific Radio Sci. Conf. (URSI AP-RASC)*, Seoul, South Korea, Aug. 2016, pp. 1–3.

[23] Italian National Research Council. (Dec. 20, 2017). *Dielectric Properties of Body Tissue in the Frequency Range 10 Hz–100 GHz*. [Online]. Available: http://niremf.ifac.cnr.it/tissprop/

[24] Y. Lee and K. Hwang, ''Skin thickness of Korean adults,'' *Surgical Radiol. Anatomy*, vol. 24, nos. 3–4, pp. 183–189, Jan. 2002, doi: 10.1007/s00276-002-0034-5.

[25] L. W. Weiss and F. C. Clark, ''Three protocols for measuring subcutaneous fat thickness on the upper extremities,'' *Eur. J. Appl. Physiol. Occupational Physiol.*, vol. 56, no. 2, pp. 217–221, Mar. 1987, doi: 10.1007/BF00640647.

[26] D. Yoon, K. Cho, and J. Lee, ''Bit error probability of M-ary quadrature amplitude modulation,'' in *Proc. 52nd Veh. Technol. Conf. Veh. Technol. Conf. Fall. IEEE VTS Fall VTC*, Boston, MA, USA, Sep. 2000, pp. 2422–2427.

[27] S.-E. Jo, J.-K. F. Suh, and Y.-J. Kim, ''Improvement of wireless power transmission efficiency of implantable subcutaneous devices by closed magnetic circuit mechanism,'' *Med. Biol. Eng. Comput.*, vol. 50, no. 9, pp. 973–980, Sep. 2012, doi: 10.1007/s11517-012-0939-z.

[28] A. Kiourti and K. S. Nikita, ''A review of implantable patch antennas for biomedical telemetry: Challenges and solutions [wireless corner],'' *IEEE Antennas Propag. Mag.*, vol. 54, no. 3, pp. 210–228, Jun. 2012, doi: 10.1109/MAP.2012.6293992.

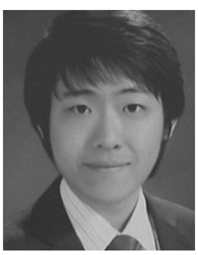

HAN-JOON KIM (S'15) received the B.S. and M.S. degrees in information control and instrumentation engineering from Kwangwoon University, Seoul, South Korea, in 2011 and 2013, respectively. He is currently pursuing the Ph.D. degree in information and communication engineering with the Daegu Gyeongbuk Institute of Science and Technology, Daegu, South Korea. His research interests include magnetic communication, wireless power transfer, and transcranial magnetic stimulation.

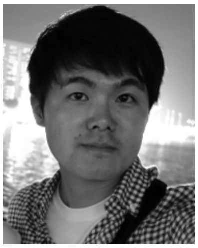

KYUNGTAE KIM received the B.S. degree in electronics engineering from Kyungpook National University, Daegu, South Korea, in 2013. He is currently pursuing the M.S. degree in information and communication engineering with the Daegu Gyeongbuk Institute of Science and Technology, Daegu, South Korea. His research interests include magnetic communication and wireless power transfer.

SUNGMIN HAN (S'13) received the B.S. degree in electronics engineering from the Korea University of Technology and Education, Cheonan, in 2012. He is currently pursuing the Ph.D. degree with the Department of Information and Communication Engineering, Daegu Gyeongbuk Institute of Science and Technology, South Korea. His research areas are communication theory and communication networks.

DONG-WOOK SEO received the B.S. degree in electrical engineering from Kyungpook National University, Daegu, South Korea, in 2003, and the M.S. and Ph.D. degrees in electrical engineering from the Korea Advanced Institute of Science and Technology, Daejon, South Korea, in 2005 and 2011, respectively. He was a Senior Researcher for the Defense Agency for Technology and Quality, Daegu, from 2011 to 2012. From 2012 to 2017, he was a Senior Researcher with ETRI, Daegu. Since 2017, he has been with the Department of Radio Communication Engineering, Korea Maritime and Ocean University, Busan, South Korea, as an Assistant Professor. His current research interests include numerical techniques in the areas of electromagnetics, radar cross-section analysis, wireless power transfer, biomedical implantable devices, and automotive radar systems.

JI-WOONG CHOI (S'00–M'04–SM'09) received the B.S., M.S., and Ph.D. degrees from Seoul National University (SNU), Seoul, South Korea, in 1998, 2000, and 2004, respectively, all in electrical engineering. From 2004 to 2005, he was a Post-Doctoral Researcher with the Inter-University Semiconductor Research Center, SNU. From 2005 to 2007, he was a Post-Doctoral Visiting Scholar with the Department of Electrical Engineering, Stanford University, Stanford, CA, USA. He was also a Consultant with GCT Semiconductor, San Jose, CA, USA, for the development of mobile TV receivers, from 2006 to 2007. From 2007 to 2010, he worked for Marvell Semiconductor, Santa Clara, CA, USA, as a Staff Systems Engineer for next-generation wireless communication systems, including WiMAX and LTE. Since 2010, he has been with the Department of Information and Communication Engineering, Daegu Gyeongbuk Institute of Science and Technology, Daegu, South Korea, as an Associate Professor. His research interests include wireless communication theory, signal processing, biomedical communication applications, and brain–machine interface.